Wind-Driven Recirculations and Exchange in the Labrador and Irminger Seas*

MICHAEL A. SPALL AND ROBERT S. PICKART

Department of Physical Oceanography, Woods Hole Oceanographic Institution, Woods Hole, Massachusetts

(Manuscript received 22 May 2002, in final form 26 November 2002)

ABSTRACT

It is demonstrated that recently observed cyclonic recirculation gyres in the Irminger and Labrador Seas may be forced by the strong cyclonic wind stress curl that develops each winter seaward of the east coast of Greenland. Idealized analytical and numerical models forced with such variable winds over a sloping bottom reproduce the essential aspects of the observed gyres (strength, location, and horizontal and vertical length scales). The communication between the forcing region in the Irminger Sea and the recirculation to the west is achieved by baroclinic topographic Rossby wave propagation along potential vorticity contours. The circulation is characterized as a time-dependent, stratified, topographic beta plume. For weak stratification, as found in the subpolar North Atlantic, the recirculation strength exhibits only weak seasonal variability, consistent with the observations, even though the forcing is active only during the winter. Baroclinic Rossby waves that develop when the wind forcing ceases in springtime interact with the bottom to provide a source of cyclonic vorticity that maintains the circulation until the wind strengthens again in the following winter.

1. Introduction

The western North Atlantic is a region of intense air–sea interaction and water mass transformation that directly influence the global overturning circulation. Warm surface waters flow into the subpolar domain, via the North Atlantic Current, and are cooled and made more dense by strong atmospheric forcing. This in turn forms intermediate waters, which ultimately exit the subpolar gyre as part of the deep western boundary current system. While this basic warm-to-cold conversion has been recognized for many years, the details of the transformation are complex, and many aspects are yet to be sorted out. Among the open issues is the precise impact of the wind-driven flow on the formation, recirculation, and export of intermediate waters.

The wintertime transformation that occurs in the subpolar North Atlantic involves the formation of mode waters and the onset of deep convection [these two may be related; see Talley and McCartney (1982)]. The former occurs throughout the subpolar gyre, producing a ''continuum'' of water mass products [akin to the formation of 18 Degree Water adjacent to the Gulf Stream: McCartney and Talley (1982)]. The latter takes place in a very limited geographical region in the Labrador Sea (Clarke and Gascard 1983), and perhaps the Irminger Sea (Pickart et al. 2003b), and forms the densest intermediate water mass in the North Atlantic—Labrador Sea Water (LSW). While mode water formation is intimately tied to the wind-driven flow of the subpolar gyre (McCartney and Talley 1982), it is less clear how the wind-forced circulation influences the formation of LSW.

Traditionally, the view is that the large-scale cyclonic wind stress curl over the western North Atlantic during fall and winter preconditions the Labrador Sea for convection (e.g., Marshall and Schott 1999). The doming of isopycnals associated with the cyclonic circulation in the interior of the basin brings dense water near the surface, exposing it more readily to the atmospheric buoyancy forcing, which in turn leads to the deep overturning. This gyre-scale circulation was thought to be very weak (order 1 cm s^{-1}), in contrast to the swift Irminger and Labrador Currents encircling the basin (e.g., Smith et al. 1937; Lazier and Wright 1993). Such a view of sluggish interior flow changed drastically, however, based on direct measurements of the middepth circulation made in the late 1990s. From an extensive dataset of Profiling Autonomous Lagrangian Circulation Explorer (PALACE) floats, Lavender et al. (2000) revealed the presence of a series of subbasin-scale recirculations embedded within the western subpolar gyre (see Fig. 1). Both the Irminger Sea and Labrador Sea contain such recirculations, which are relatively strong (order 5 cm s^{-1}), narrow (order 300 km), and weakly baroclinic below 400 m (see Lavender et al. 2000; Pickart et al. 2002). Their dynamic pressure anomaly is O(2–

* Woods Hole Oceanographic Institution Contribution Number 10664.

Corresponding author address: Dr. Michael A. Spall, Dept. of Physical Oceanography, Woods Hole Oceanographic Institution, MS #21, Woods Hole, MA 02543.
E-mail: mspall@whoi.edu

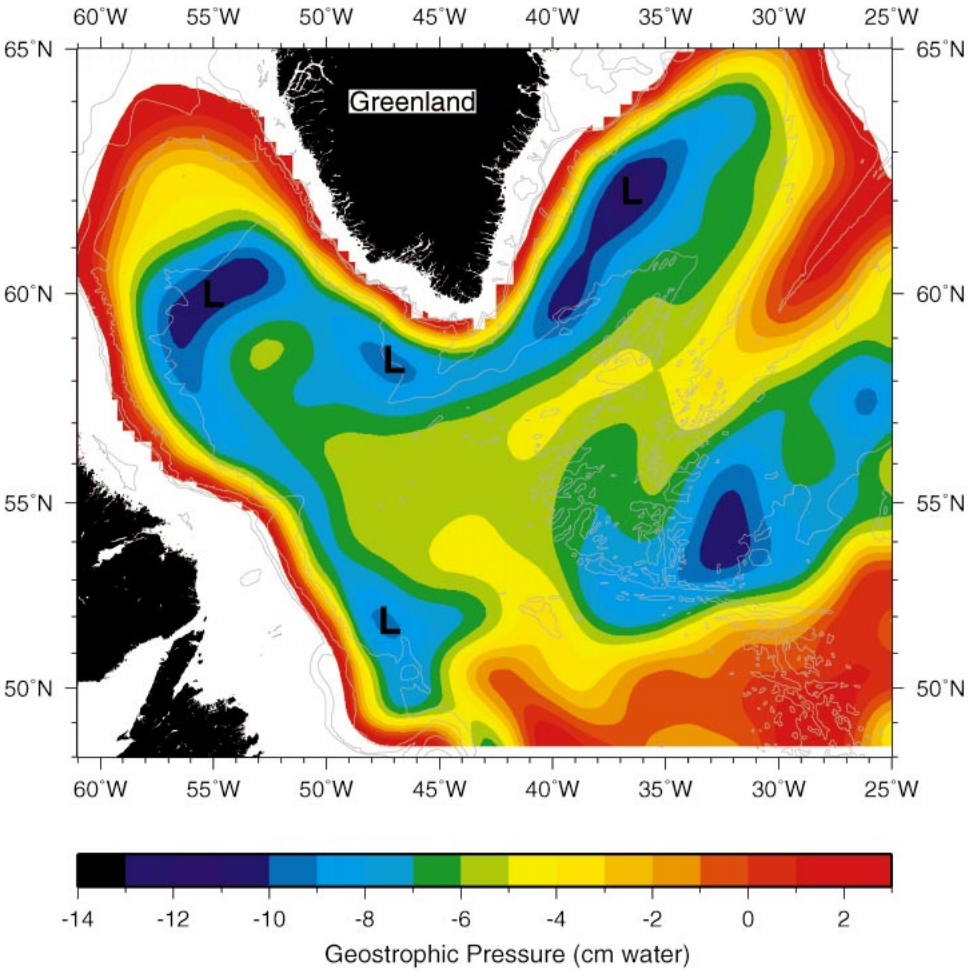

FIG. 1. Geostrophic pressure anomaly at 700-m depth (after Lavender et al. 2000) showing a series of cyclonic recirculations (darker blue, denoted L for low pressure) adjacent to the continental slope. The bathymetric contours are 500, 1000, 2000, and 3000 m.

4 cm) and their transport is approximately 2–5 Sv (Sv $\equiv 10^6$ m^3 s^{-1}). Furthermore, the gyres seem to be present year-round, with apparently little seasonal dependence.[1]

Recent hydrographic evidence suggests that these recirculations may play a key role in the formation and export of LSW. A 1997 wintertime survey of the Labrador Sea revealed that the deepest convection occurred within the trough of the gyre in the western portion of the basin (Pickart et al. 2002). This was corroborated by the PALACE float profile data collected over consecutive winters (Lavender 2001). The same seems to hold in the Irminger Sea, where vertical profiles of density stratification indicate that the deepest wintertime overturning occurs within the cyclonic recirculation east of Greenland (Pickart et al. 2003b). Apparently, these closed gyres enable the necessary preconditioning for deep convection to occur by locally trapping the water in areas of high surface buoyancy loss, akin to what happens in the western Mediterranean (Madec et al. 1996). The gyres also impact the spreading of LSW after formation, both in terms of timing and pathways (Straneo et al. 2003).

At present, the nature and cause of the subbasin-scale recirculations in the Labrador and Irminger Seas are largely unknown. The recent study by Käse et al. (2001) suggests that wind forcing, overflows, and bottom topography all play important roles. Nonetheless numerous questions remain. What, specifically, are the driving mechanisms? What sets the strength and spatial scales of the recirculations? Are they seasonally variable? Are they specific to this region? If we are to understand fully the process of convection and water mass transformation

[1] Clarke and Gascard (1983) reported interior velocities comparable to those observed by the PALACE floats, which they attributed to a buoyancy-forced wintertime gyre in the western Labrador Sea. The baroclinic shear associated with this seasonal feature is very weak (Pickart et al. 2002). We suspect that Clarke and Gascard (1983) were in fact measuring the same year-round, wind-driven flow discussed in the present paper.

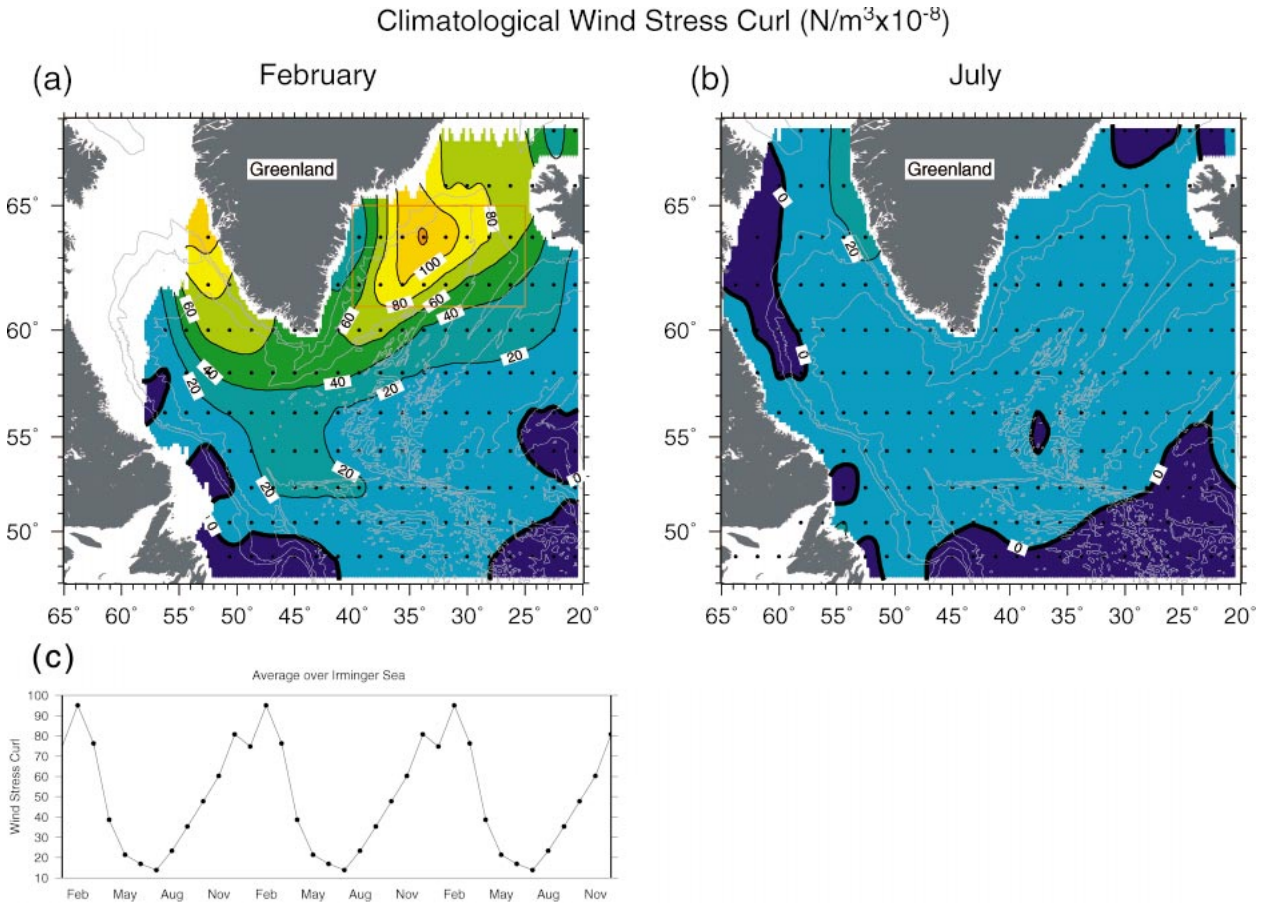

FIG. 2. Climatological wind stress curl calculated from the NCEP reanalysis product for the period from 1979 to 1998 (Renfrew et al. 2002) for (a) Feb and (b) Jul. The bathymetric contours are 1000, 2000, and 3000 m. (c) Monthly mean wind stress curl in the Irminger Sea, averaged over the region denoted by the red box on (a).

in the subpolar domain, it is clear we must learn more about these recirculations. The present paper attempts to do this. In particular, we argue that the wind field in the vicinity of Greenland plays a dominant role in forcing the gyres in both the Irminger and Labrador Seas. Using a hierarchy of models we demonstrate how seasonally varying winds drive a persistent interior recirculation in the presence of sloping topography and weak stratification. The appropriate dynamics are those of a stratified, topographic beta plume, and the predicted structure, strength, and scales of the recirculations agree well with the observations. We begin with a description of the wind-driven gyres, followed by an analysis of their dynamics. Some parameter sensitivities are demonstrated next, and last we discuss possible differences in the forcing mechanisms in the Labrador and Irminger Sea recirculations.

2. Wind-driven circulations

The winter winds in the vicinity of Greenland result in some of the strongest wind stress curl found anywhere in the World Ocean (Milliff and Morzel 2001). While values over most of the subpolar North Atlantic are $O(10^{-7}\ \mathrm{N\ m^{-3}})$, in winter intense cyclonic wind stress curl is found on both sides of Greenland that exceeds $10^{-6}\ \mathrm{N\ m^{-3}}$ (see Fig. 2). This is due to the wintertime low pressure systems that transit through the region. [Often the same storm influences the Labrador Sea first, then the Irminger Sea a few days later (see, e.g., Pickart et al. 2003a).] The resulting curl pattern appears in the winter climatological mean of the National Centers for Environmental Predicition (NCEP) reanalysis (Fig. 2a), as well as the European Centre for Medium-Range Weather Forecasts (ECMWF) analysis (see Trenberth et al. 1989). The spatial pattern and strength of this signal do not seem to depend strongly on whether the North Atlantic Oscillation (NAO) index is high or low (Pickart et al. 2002); thus it appears to be a regular feature of the wind-forcing in this region.[2] As indicated in Figs. 2b and 2c, the amplitude of the wind stress curl varies strongly with season. The forcing is enhanced through-

[2] This is in contrast to the heat flux over the western subpolar North Atlantic, which is strongly modulated by the NAO.

out the winter months, with the strongest curl occurring in February. The forcing then decreases by an order of magnitude through the spring, and by summer the wind stress curl is essentially indistinguishable from the large-scale values found throughout the subpolar gyre (Fig. 2b).

One immediately notices that the spatial scales of the extrema in wind stress curl are comparable to the width of the observed recirculation gyres found in the Labrador and Irminger Seas (Fig. 1). Furthermore, the strongest recirculation appears in the region of strongest wind stress curl east of Greenland. The cyclonic sense of the recirculation is consistent with what is expected for this sign of wind forcing, which induces upwelling. One also sees that the along-slope scale of the recirculations is much larger than the cross-slope scale. This is expected for a localized region of upwelling and weak dissipation, as originally outlined by Stommel (1982) as a mechanism for the generation of Helium plumes in the South Pacific (the so-called beta plume). However, while the general characteristics of the recirculation gyres are consistent with this type of forcing, it is not clear what effect time-dependent winds, stratification, and bottom topography might have on the mean and time-dependent oceanic circulation.

We have chosen to focus this initial study on the effects of the enhanced wind stress curl in the vicinity of Greenland on the circulation in the Labrador and Irminger Seas. Other aspects of the subpolar gyre circulation are neglected, including the component of the boundary current system driven by the basin-scale subpolar winds (i.e., the Sverdrup return flow) as well as the thermohaline circulation. This approach, while idealized, allows us to explore in some detail the dynamics of the oceanic response to such localized, seasonal forcing. It is possible that these neglected components of the general circulation may interact with the circulations studied here in interesting and important ways; however, we feel that it is prudent to understand the consequences of the intense localized wintertime winds in isolation before considering such additional complications.

It should be kept in mind that both the NCEP and ECMWF fields are at relatively low resolution [O(100–200 km)], and hence they represent the moderate-scale (but smaller than basin-scale) atmospheric forcing in the region. Phenomena at even smaller scales than this, for instance local winds associated with the fjords and steep topography of Greenland, are not adequately resolved by these global weather products (Pickart et al. 2003a). Such features may force oceanic currents in addition to the larger-scale circulations being studied here.

a. Model configuration

We explore the oceanic response to seasonal, spatially variable wind forcing, as is found east of Greenland, using the Massachusetts Institute of Technology (MIT) Ocean General Circulation Model (Marshall et al. 1997a,b). The hydrostatic, primitive equation version of the model is used, because the spatial scales of the forcing and oceanic circulation are large in comparison with the depth of the ocean. No surface buoyancy flux is applied so that convective overturning does not occur. This model is well suited for the problem at hand since it uses a partial-cell representation of the bottom depth, which has been shown to be more accurate than the stair-step bottom topography traditional to level coordinate models (Adcroft et al. 1997). The level vertical coordinate system also allows for an accurate treatment of the lateral pressure gradient terms in the momentum equations, an important attribute for stratified flow over steep topography.

The model is configured in an idealized basin crudely representing the Irminger and Labrador Seas. The domain is 1200 km by 900 km with a peninsula extending 275 km southward from the northern boundary (the model equivalent of Greenland), as shown in Fig. 3. The horizontal grid resolution is 7.5 km, and there are eight levels uniformly distributed in the vertical (375 m thickness). The bottom depth decays exponentially away from the northern and western boundaries to a maximum depth of 3000 m, with an e-folding scale of 60 km. The Coriolis parameter varies linearly with latitude as $f = f_0 + \beta^*(y - y_0)$, where $f_0 = 1.2 \times 10^{-4}$ s^{-1} is the Coriolis parameter at y_0, the midlatitude of the domain, and $\beta^* = 2 \times 10^{-13}$ cm^{-1} s^{-1}. The model has Laplacian horizontal temperature diffusion and viscosity, with coefficients of 20 and 50 m^2 s^{-1}, respectively. The vertical diffusion and viscosity coefficients are 10^{-5} m^2 s^{-1}.

We force the model with a localized patch of positive wind stress curl to the east of Greenland. Note in Fig. 2a that the maximum curl in the Irminger Sea is stronger than that in the Labrador Sea, and is also located over deeper topography where the observed recirculation is strongest (Fig. 1). The pattern and maximum amplitude of the model wind stress curl is shown superimposed on the bottom topography in Fig. 3. It is strongest over the continental slope and decays in both the zonal and meridional directions. This pattern is consistent with the February wind stress curl calculated from the NCEP reanalysis shown in Fig. 2. We explore the effects of the weaker wind stress curl maximum to the west of Greenland in section 5. The seasonal cycle is imposed through modulating the amplitude of the curl as a function of time (Fig. 4). We use a Gaussian with a decay scale of 60 days so that the amplitude peaks in winter and decays to zero during the summer—representative of that found in the NCEP reanalysis.

The model is initialized at rest with a uniform stratification and run for a period of 10 years. It takes approximately this long for a first mode baroclinic Rossby wave to cross the basin, so at this point the annual mean circulation is nearly steady. The model uses a linear equation of state and constant salinity so that density is linearly proportional to temperature. For most cases the

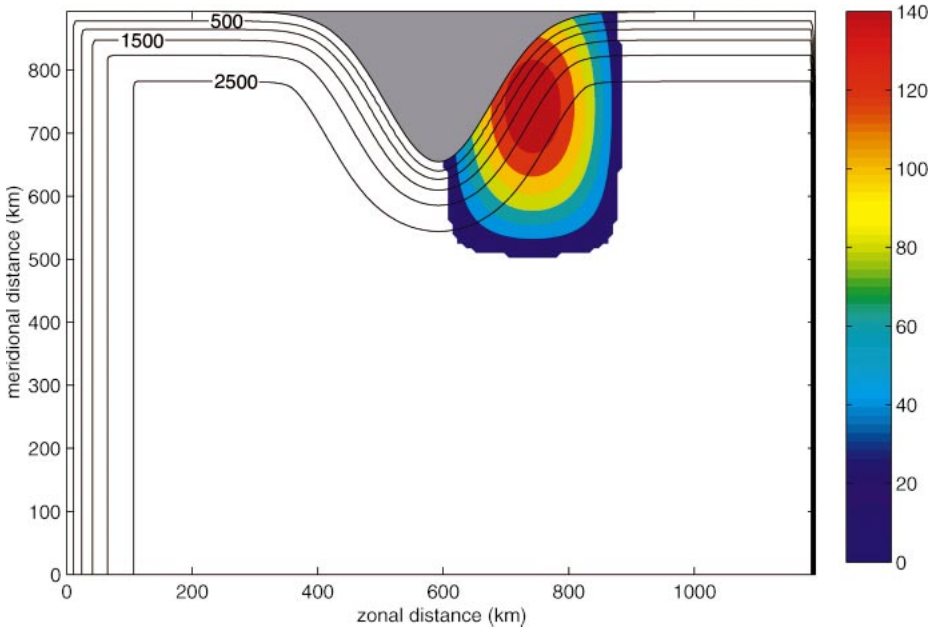

FIG. 3. Model bottom topography (contours) and wind stress curl forcing (N $m^{-3} \times 10^{-8}$).

initial stratification is such that the first baroclinic deformation radius $\sqrt{\Delta\rho H}/f_0 = 20$ km, where $\Delta\rho$ is the change in density from the surface to depth H and $H = 3000$ m is the maximum water depth.

b. Mean circulation

The annual-mean sea surface height from the final year of integration is shown in Fig. 5. The dominant feature is a large-scale cyclonic circulation extending from the forcing region (east of Greenland) cyclonically around the Labrador Sea. The flow follows the topography around the southern tip of Greenland, into the Labrador Sea, and then equatorward along the continental slope. The flow along the western boundary extends well south of the latitude of forcing. (The large-scale pattern is not significantly influenced by the solid boundary to the south.) In the southwest portion of the domain the flow retroflects and turns eastward from the western boundary. Once over the flat bottom in the interior, the flow is nearly zonal until encountering the region of wind stress curl east of Greenland. Under the influence of surface forcing, the flow turns to the north and closes the recirculation. A region of local minimum sea surface height is located to the south and east of Greenland.

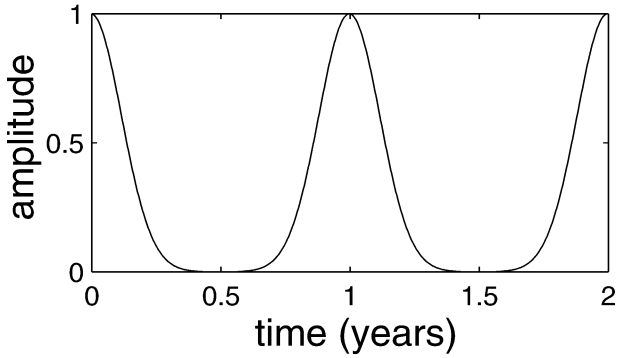

FIG. 4. Seasonal modulation of the strength of the wind stress curl.

This general pattern of the mean circulation contains many of the essential characteristics of the middepth circulation revealed by the PALACE float study of Lavender et al. (2000). The observed circulation is dominated by westward and equatorward flow along the topography, a retroflection in the southwestern Labrador Sea, and eastward flow in the interior south of Greenland. The minimum pressure is found east of Greenland in both the model and the observations. The float data indicate more closed contours here, but this may be a result of the idealized forcing and topography used in the model or uncertainties in the data. The amplitude of the pressure minimum east of Greenland in the model (relative to the pressure in the interior of the Irminger Sea) is approximately 2.5 cm, similar to that inferred from the float data. The major discrepancy between the model and data is the lack of closed contours in the northern Labrador Sea in the model, in contrast to the strong cyclonic recirculation in the observations. We return to this feature in section 5. Within reasonable uncertainties in the objectively mapped float data [O(1 cm) in dynamic pressure], the model pressure agrees well with the observations in both pattern and amplitude.

The recirculation in Fig. 5 is consistent with a beta-plume circulation forced by a localized region of steady

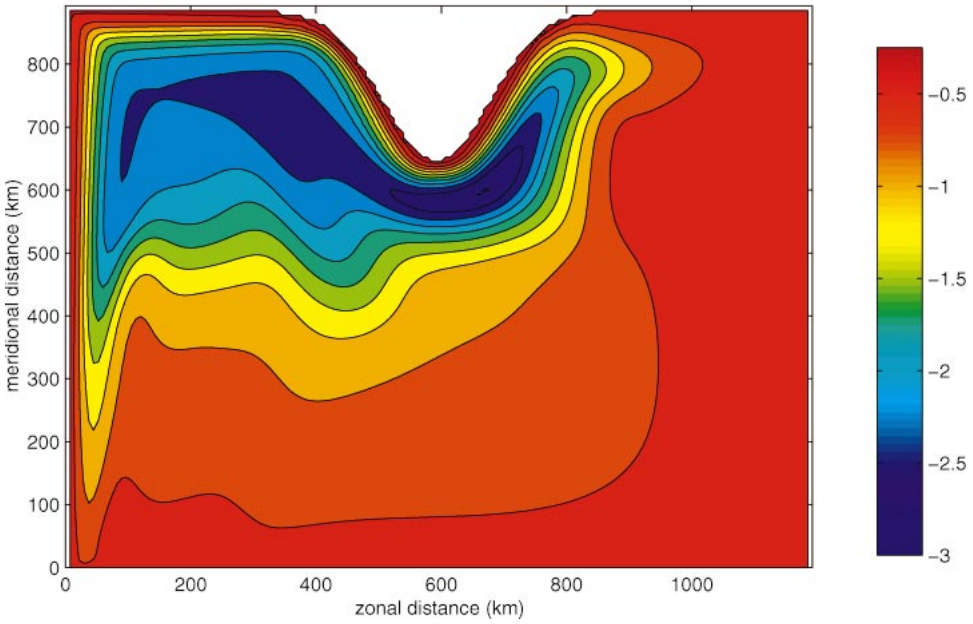

FIG. 5. Mean sea surface height anomaly (cm) from the final year of the standard-case 10-yr integration.

upwelling (Stommel 1982). In this case the upwelling is provided by the cyclonic wind stress curl and the resulting Ekman suction. In the standard beta-plume model, the region under the forcing obeys a linear, Sverdrup balance such that vorticity input from the wind is balanced by flow across planetary vorticity contours. Outside of the region of direct wind forcing and away from viscous boundary layers, the flow is along contours of constant potential vorticity. In the case of a flat bottom, this is dictated by the planetary vorticity and the flow is zonal. For steep topography and weak stratification, as is the case here, the potential vorticity contours extending to the west from the forcing region are dominated by the bottom topography. However, the region along the western boundary supports a viscous boundary layer so that the flow is forced to cross potential vorticity contours as it flows to the south. The degree of dissipation experienced along the western boundary is a function of both boundary layer width and slope of the bottom topography. For a region of topographic slope wider than the viscous boundary layer, the sloping bottom will result in less dissipation than will a flat bottom. This causes the equatorward flow to overshoot its equilibrium latitude as it flows southward and retroflect before leaving the western boundary. Once in the interior, the dissipation is weak and the eastward flow is along planetary vorticity contours. A similar overall pattern is found for free-slip boundary conditions (not shown), but the southward flow along the western boundary flows briefly eastward along the southern wall of the domain before returning to the north because there is less dissipation in the western boundary region.

This elongated recirculation pattern is very different from the localized recirculation forced by wind stress curl of both signs presented by Madec et al. (1996) in their study of the Mediterranean Sea. In their case, the spatially averaged vorticity input by the wind is zero, and so there is no need to dissipate vorticity in a strong boundary current. The potential vorticity balance is achieved by advecting water parcels directly from the region of cyclonic wind stress curl into the region of anticyclonic wind stress curl. This results in an oceanic circulation that is of the same spatial scale as the wind forcing. Because the wind forcing in our case is of a single sign, the only way in which the vorticity budget can be balanced is through the development of a viscous boundary layer. For the moderate values of lateral dissipation used here, the only place where significant dissipation can develop is near the western boundary of the Labrador Sea. (While a small amount of dissipation also occurs along the east coast of Greenland, the slanted coastline and bottom topography limit the amount of dissipation found there.) For wind forcing that is located away from the western boundary, the spatial scale of the resulting oceanic circulation is much larger than the scale of the wind itself. The fact that the dissipation region is remote from the forcing region is also important for the timescale of the oceanic adjustment, which is set by the time it takes a baroclinic Rossby wave to propagate from the area of forcing to the area of dissipation. For the subpolar North Atlantic this can be many years, as discussed below.

The structure and driving mechanism of the recirculation of Fig. 5 also differ significantly from those recently described by Käse et al. (2001). They used a series of models, configured for the northern North Atlantic and forced with winds derived from an adjoint

data assimilative model and/or overflows, to produce recirculations along the boundaries of the Labrador and Irminger Seas. Although there are some elements in common, such as wind forcing and topography, our results differ from theirs in several fundamental ways. First, we assign the primary forcing of these recirculations to the specific winds along the east coast of Greenland during the winter, although we do not rule out the possibility that local winds may enhance the recirculations in the Labrador Sea (see section 5). By contrast, Käse et al. (2001) indicate that their recirculations are due to wind forcing all along the boundaries and that the northern overflows also play an important role in determining the strength of the recirculations. Furthermore, our recirculations have maximum velocities of O(2–4 cm s^{-1}) and transports of O(2–3 Sv)—consistent with the observations of Lavender et al. (2000)—whereas the Käse et al. (2001) recirculation gyres are much stronger, with velocities in excess of 15 cm s^{-1} and transports of O(20 Sv). Last, our recirculations are strongest to the east of Greenland, while theirs are strongest along the western boundary of the Labrador Sea.

c. Seasonal variability

The float data suggest that this general pattern is present in all seasons (Lavender 2001). The forcing in our model varies strongly with the season, so it is of interest to look at the strength of the circulation versus time of year. The general pattern of sea surface height looks similar to the mean throughout the year. The primary change is a slow propagation toward the west of the location of the minimum sea surface height after the wind forcing has peaked in winter. For the stratification and topography used here, the local minimum propagates only about 150 km toward the west (just to the west of the southern tip of Greenland) by the following winter, when the wind forcing increases again and enhances the sea surface height signal under the forcing region.

The amplitude of the pressure and, hence, the strength of the circulation vary with time of year. This is best demonstrated by a time series of the minimum sea surface height in the Irminger and Labrador Seas, as shown in Fig. 6a for the last 2 years of integration. The minimum sea surface height in the Irminger Sea (defined as the region east of 600 km longitude and north of 600 km latitude) fluctuates around −2.5 cm, with a seasonal variability of approximately 1 cm. The sea surface height in the Labrador Sea is taken as the minimum value within 300 km of the western boundary at latitude 700 km. The mean and seasonal amplitude in the western Labrador Sea are very similar to, but slightly less than, that found in the Irminger Sea. Although there is a clear seasonal signal in both seas, the change in sea surface height over the year is much less than the mean value. As a result, a low pressure signal exists in both

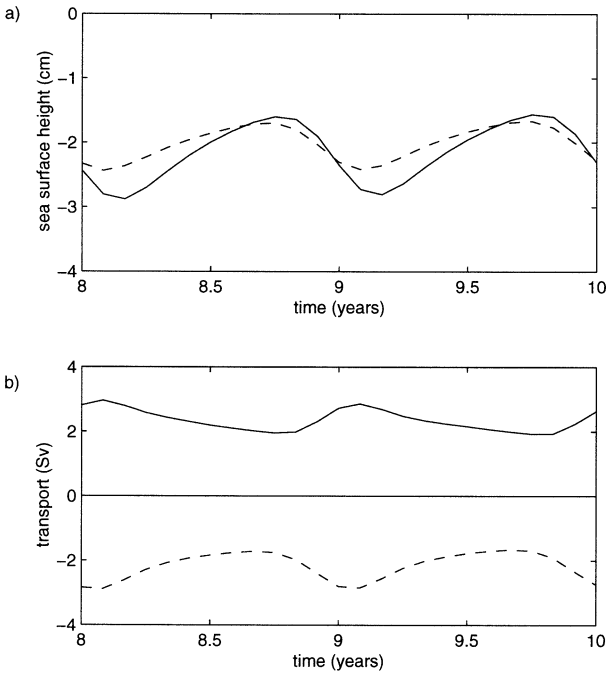

FIG. 6. Time series of (a) minimum sea surface height anomaly in the Irminger (solid) and Labrador (dashed) Seas and (b) eastward transport south of Greenland (solid) and southward transport in the western Labrador Sea (dashed) over the final 2 yr of integration.

basins all year long, even though the forcing is active only during the winter months. When the wind is turned on, the sea surface height decreases, reaching its minimum value when the wind ceases in spring. Subsequent to this, the sea surface height slowly begins to increase toward zero. Such a small seasonal cycle suggests that it might be difficult to discern any clear seasonality in PALACE float data that are irregular in space and time.

One of the important aspects of the circulation pattern revealed by Lavender et al. (2000) is the presence of an eastward flow, just south of Greenland, from the Labrador Sea into the Irminger Sea. This may provide a direct and relatively rapid means to advect recently ventilated waters from the western Labrador Sea into the Irminger Sea and eastern subpolar gyre (see Sy et al. 1997; Straneo et al. 2003). The amplitude of this eastward transport, integrated over the whole water column in the model, is shown in Fig. 6b over the final 2 years of integration. The transport into the Irminger Sea is present year-round with a mean value of 2.2 Sv and a seasonal variation of approximately ±0.5 Sv. The corresponding flow of water into the Labrador Sea, and its seasonal cycle, is characterized by the southward transport along the west coast of the Labrador Sea at latitude 700 km, shown in Fig. 6b by the dashed line. The maximum transport is found just after winter and the minimum transport is in autumn, but the general sense of the circulation is present year-round.

The mean eastward transport calculated from the Lavender et al. (2000) PALACE float data at the southern

tip of Greenland is approximately 3.3 ± 1 Sv (Lavender 2002, personal communication). The maximum transport in the data is found in spring, but given the relatively low amount of data when the floats are subdivided into seasons, estimates of the seasonal cycle are subject to large uncertainties. Nonetheless, the magnitude of the transport based on the observations is close to the transport produced in the model, especially considering the very idealized nature of the model forcing and configuration.

In a general sense, the large-scale recirculation found in the numerical model is qualitatively similar to the steady beta-plume circulations discussed by Stommel (1982), Pedlosky (1996), and Spall (2000). However, we have added several complicating factors, including time-dependent forcing, stratification, topography, and a complex coastline. In the next section, we develop a simple analytic solution that helps in understanding how these factors influence the mean strength, time dependence, and pathways of the circulation.

3. Dynamics of stratified, topographic beta plumes

It is useful to first review the steady circulation resulting from localized upwelling over a flat bottom. The beta-plume circulation may be broken down into three dynamical regimes. The first is the forcing region, in which the balance is between vorticity input from the wind (or upwelling) and advection across the mean vorticity gradient. For upwelling, the flow in the forcing region is toward the pole. Outside of the latitude range of the forcing and away from meridional boundaries (the second dynamical regime) the flow must be zonal. Neglecting eastern boundary layers, this results in a westward flow just poleward of the forcing region, and a returning eastward flow equatorward of the forcing region. These zonal flows are along contours of constant potential vorticity because both the forcing and the dissipation are assumed weak. Last, the circulation is assumed to close somewhere to the west in a viscous boundary layer (the third dynamical regime). It is important to note that the region of dissipation can be far from the region of forcing, yet the strength of the recirculation is controlled by the meridional transport under the region of the winds.

a. Two-layer quasigeostrophic model

If we can shed light on what controls the transport in the forcing region, then the basic response of the large-scale recirculation can be understood directly as a result of mass continuity. The essential dynamics of the oceanic response to such localized, seasonal forcing events in the presence of stratification and bottom topography are made clearer through consideration of a simple two-layer, two-dimensional quasigeostrophic (QG) system. For simplicity, we assume in this model that the bottom topography slopes uniformly upward to the north and that the forcing is independent of latitude. This is meant to correspond in the simplest setting possible to the first dynamical region noted above, that is, the region directly subject to the wind stress curl. The correspondence of this simple configuration to the more complex bottom topography and realistic forcing of the Irminger and Labrador Seas is demonstrated in section 3b through use of the primitive equation numerical model.

In the QG framework, the nondimensional potential vorticity equation for each layer may be written as

$$-F_1(\psi_1 - \psi_2)_t + \beta\psi_{1x} = \tau, \tag{1}$$

$$F_2(\psi_1 - \psi_2)_t + (\beta + \alpha)\psi_{2x} = 0. \tag{2}$$

The upper-layer streamfunction is ψ_1, the lower-layer streamfunction is ψ_2, $\beta = \beta^* L^2/U$, $\alpha = f_0 h_y L^2/(Uh)$, h_y is the bottom slope, h is the mean bottom depth, and U and L are the characteristic horizontal velocity and length scales. The stratification parameters are $F_i = f_0^2 L^2/(g' H_i)$, where f_0 is the Coriolis parameter; g' is the reduced gravity, and H_i is the thickness of layer i. The wind stress curl forcing τ is active in the upper layer only. It has been assumed that the dominant length scales are large in comparison with the internal deformation radius, and so the relative vorticity contribution to potential vorticity is negligible. Subscripts t and x indicate partial differentiation with respect to time and the zonal direction.

Equations (1) and (2) can be manipulated to form a single equation for the baroclinic shear $\Psi = \psi_1 - \psi_2$,

$$F\Psi_t - \beta\Psi_x = -\tau. \tag{3}$$

The stratification parameter is now $F = F_1 + F_2[1 - \alpha/(\beta + \alpha)]$. The influence of bottom topography is represented by the ratio $\alpha/(\beta + \alpha)$. For very weak bottom slopes, $F \approx F_1 + F_2$, and the upper-ocean and deep-ocean stratifications are evenly weighted. However, the upper ocean becomes isolated from the bottom as the bottom slope increases. For very strong bottom slopes $F \approx F_1$ and the deep stratification and bottom slope become unimportant for the baroclinic shear Ψ.

The streamfunction in the second layer is related to Ψ as

$$\psi_{2x} = -\frac{F_2\Psi_t}{\beta + \alpha}. \tag{4}$$

Equation (3) may be solved using the method of characteristics. To obtain a solution, one must specify the value of Ψ on all characteristics where they enter the domain, in this case at the eastern edge of the forcing region, and integrate the changes in Ψ as a result of wind forcing along the characteristic trajectory. For simplicity, it is assumed here that there is no flow east of the forcing region so that $\Psi(x = 0) = 0$. The characteristic paths propagate directly westward at the baroclinic Rossby wave phase speed, $\partial x/\partial t = -\beta/F$. For weak stratification, $F \gg 1$ and this propagation is slow,

while for strong stratification $F \ll 1$ and this propagation is fast. If the distance along a characteristic is given by s, then Ψ changes along the characteristic in response to the wind forcing as $\partial\Psi/\partial s = -\tau$. If there is no wind forcing, then the value of Ψ remains constant along that segment of the characteristic path.

For steady forcing, a critical characteristic exists that separates that part of the ocean still adjusting to the wind forcing and that part in which the circulation is steady (Anderson and Killworth 1977). This characteristic originates at the eastern edge of the forcing region and propagates westward at the baroclinic Rossby wave phase speed. To the west of this characteristic, the zonal gradient of Ψ is zero, and Ψ grows linearly in time as $\partial\Psi/\partial t = -\tau/F$. The critical characteristic passes location x at time $t = -xF/\beta$ after which the solution is steady, given by the Sverdrup balance:

$$\psi_1 = \frac{\tau x}{\beta}, \qquad \psi_2 = 0. \tag{5}$$

For weak stratification, this spinup takes a long time, while for strong stratification the solution reaches equilibrium quickly.

The essential response to strong forcing in winter and weak or no forcing in summer is revealed through application of a step function in the strength of the wind stress curl. We consider a case in which the wind forcing is of constant strength τ_0 for duration Δ, and inactive for duration $P - \Delta$. This forcing is continuously repeated so that the period of the forcing is P.

If much of the forcing region lies to the west of the critical characteristic that separates the time-dependent region from the steady region, the circulation will not equilibrate before the forcing changes. Characteristics will propagate a distance $\beta\Delta/F$ while the wind forcing is active. For parameters representative of the Irminger and Labrador Seas, say 20-km internal deformation radius and 90 days of forcing, this distance is O(60 km). The width of the forcing region to the east of Greenland is several hundred kilometers, and so we anticipate that most of the forcing region will lie to the west of the critical characteristic.

The solution following a characteristic trajectory that lies to the west of the critical characteristic may be written as

$$\Psi(s, t) = \Psi_0 - \tau_0 t/F, \tag{6}$$

where Ψ_0 is the value of Ψ on this characteristic when the wind forcing is turned on (at time $t = 0$). The value of Ψ following the characteristic remains constant when the wind forcing is off. Before presenting the solution for Ψ, several useful quantities can be determined from (6). The mean value of Ψ at a fixed location x (i.e., not following a trajectory) may be derived by recognizing that, when the system has reached a quasi-equilibrium state, the change in Ψ over period P must be zero. During the winter, when the wind forcing is active, the change in Ψ is $-\tau_0\Delta/F$. This is offset over the remainder of the year by the westward propagation of the baroclinic Rossby waves. The change in Ψ due to wave propagation may be written in terms of the zonal gradient of Ψ and the characteristic speed as

$$-\frac{\partial\Psi}{\partial x}\frac{\partial x}{\partial t}P = \frac{\beta\overline{\Psi}P}{Fx}. \tag{7}$$

We approximate the zonal gradient of Ψ as $\partial\Psi/\partial x = \overline{\Psi}/x$, where $\overline{\Psi}$ is the mean value of Ψ at location x. It has been assumed here that $\Psi = 0$ at the eastern edge of the wind forcing. In the quasi-equilibrated state, the change in Ψ during the winter must be balanced by the change in Ψ due to westward Rossby wave propagation so that the mean value of Ψ at location x is

$$\overline{\Psi} = \frac{\tau_0 x\Delta}{\beta P}. \tag{8}$$

Although the lower layer is generally in motion throughout the year, the annual mean of the lower-layer streamfunction is zero because, in the quasi-equilibrium state, there is no change in Ψ over time period P so, by (4), $\overline{\psi}_{2_x} = 0$. The annual-mean upper-layer streamfunction is just the steady Sverdrup transport weighted by Δ/P, the fraction of time that the wind is active. These layer solutions are expected because in this linear, inviscid model there are no eddy fluxes of potential vorticity, so the mean solution for time-dependent forcing must equal the steady solution for the mean of the forcing.

The ratio of the change in Ψ during the winter, $\delta\Psi$, to its annual mean value $\overline{\Psi}$ is an indication of the relative strength of the seasonal cycle. This ratio may be written as

$$\frac{\delta\Psi}{\overline{\Psi}} = \frac{\beta P}{Fx}. \tag{9}$$

The quantity $\beta P/F$ is the distance a baroclinic Rossby wave propagates over the time period P. If this distance is small in comparison with the width of the forcing region, then the change in circulation from winter to summer will be small in comparison with the mean circulation strength. For the value of the deformation radius used above (20 km), the ratio (9) is less than 1, implying a weak seasonal cycle. This is consistent with the results of the previous section whereby the seasonal cycle in the primitive equation model is much less than the annual mean.

The sense of the circulation produced by such seasonal forcing is now demonstrated. We take a deformation radius of 20 km, uniform bottom slope of 10^{-3}, and a maximum bottom depth of 2500 m, so that $\alpha = 5\beta$. The wind forcing is turned on for 90 days and turned off for 270 days per year. The nondimensional meridional velocity under the forcing region from the analytic solution to (3) and (4) is shown in Fig. 7 over the final 2 yr of a 10-yr integration. While the wind is active, the meridional velocity in both layers is toward the north

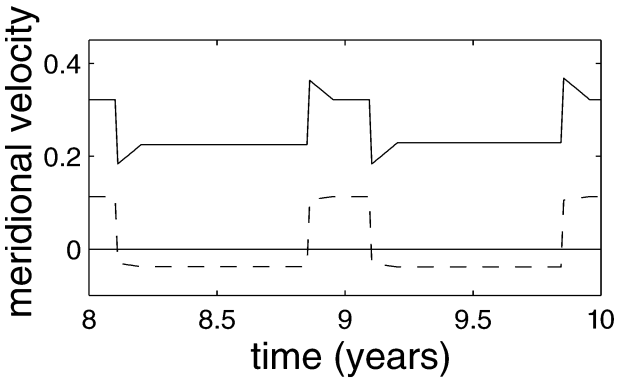

FIG. 7. Nondimensional northward velocity in the upper (solid) and lower (dashed) layers from the two-layer quasigeostrophic theory. The flow is northward in both layers when the wind is active. The flow remains northward in the upper layer but reverses to the south in the deep layer when the wind is off.

and is about 3 times stronger in the upper layer than it is in the lower layer. During the summer months, when the wind is off, the upper-layer flow remains northward at about two-thirds of its winter strength, while the lower-layer flow is weak and toward the south. There is a net northward flow when integrated over the entire water column at all times of the year.

This simple model indicates that the cyclonic circulation forced by the wind in winter can persist all year long, provided that the Rossby waves propagate slowly. The key to understanding how the cyclonic circulation is maintained, even when there is no active forcing, lies in the deep ocean. The zonal gradient of the lower-layer streamfunction, and hence the deep meridional flow, is proportional to the time rate of change of Ψ by (4). During winter, Ψ becomes increasingly negative due to the active wind forcing. The zonal gradient of the deep streamfunction is then positive, indicating a northward flow near the bottom. Because the bottom slopes upward, this gives rise to compression at the bottom that partially offsets the stretching forced by the wind at the surface. The resulting meridional flow is weaker than what would be forced over a flat bottom. During the summer, when the wind forcing is absent, Ψ increases in time as a result of westward propagation. The zonal gradient of the lower-layer streamfunction is then negative, giving rise to southward flow and stretching at the bottom. This provides a source of cyclonic vorticity to the water column and maintains the same sense of circulation as the wind forcing in winter. The combined effect of the bottom topography and stratification weaken the upper-ocean cyclonic response to the wind in the winter and maintain the cyclonic circulation during the summer when the wind is off.

b. Primitive equation model

The relevance of the simplified two-layer quasigeostrophic theory presented above to the full three-dimensional circulation is now demonstrated by comparing the solution from (3) and (4) directly with the MIT model. In this case, the MIT model is configured and forced as the previous QG model. The numerical model has uniform stratification (deformation radius 20 km) with eight levels uniformly distributed in the vertical (thicknesses of 312.5 m). The model domain is 960 km by 960 km with horizontal grid spacing of 15 km. The maximum bottom depth is 2500 m and the bottom depth decreases uniformly toward the north with slope 10^{-3}. The seasonal wind forcing is applied over a region in the eastern portion of the domain, as indicated in Fig. 8 (recall that the QG model applies to this region only). The annual-mean sea surface height (Fig. 8) shows the expected cyclonic recirculation. The surface flow in the forcing region is predominantly meridional, with nearly zonal flows extending westward from the northern and southern limits of the forcing region. The viscous western boundary layer allows for a southward return flow along the western boundary. There is no overshoot, as found for the more realistic topography case, because the topography is perpendicular to the boundary.

The time-dependence of this idealized calculation is now compared with the two-layer quasigeostrophic theory. The meridional velocity in the MIT primitive equation model in the forcing region is shown in Fig. 9 over the same 2-yr period (a weak time filter has been applied to suppress rapid oscillations due to barotropic Rossby waves that are excited by the sudden onset of the winds). The overall flow is very similar to that predicted by the theory (cf. Fig. 7). The velocity is northward in both layers while the wind is active and, when the wind is off, the upper layer continues to flow toward the north while the lower layer becomes weak and reverses to the south. The connection between the meridional flow under the forcing region and the recirculation to the west of the forcing region is demonstrated by mean zonal flow in level 1 to the west of the forcing region (at $x = 270$ km, indicated by the dashed line in Fig. 8). The zonal flow is of similar magnitude to the meridional flow under the forcing region and exhibits only a slight phase lag. This confirms that the transport and phase of the large-scale recirculation to the west of the forcing region is directly controlled by the flow under the region of forcing. This justifies the use of the simple two-dimensional analytic model to expose the underlying dynamics of the system.

4. Sensitivity to topography and stratification

The quasigeostrophic theory indicates that the strength of the seasonal cycle should be strongly dependent on the stratification of the water column [from (9)]. To investigate this, we have carried out two additional calculations using the MIT model with the forcing and domain as in Fig. 3, except that the basic stratification has been increased by factors of 2 and 4. The resulting deformation radii are 28 and 40 km. The sea

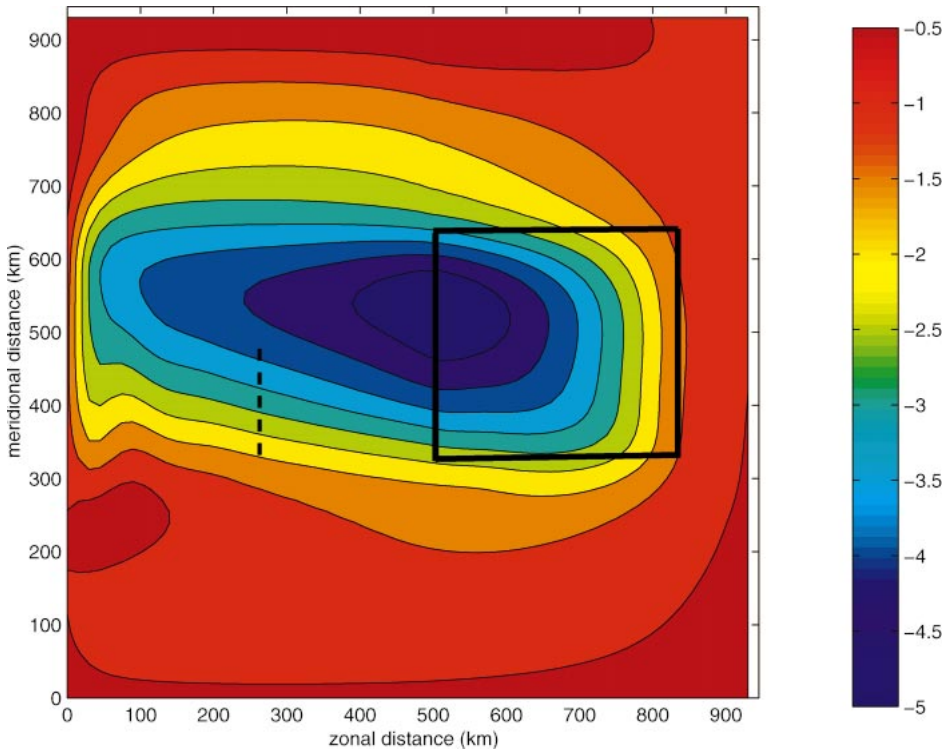

FIG. 8. Annual mean sea surface height anomaly (cm) after 10 yr of integration for the idealized beta-plume calculation. A uniform wind stress curl is applied over the region indicated by the square, while the zonal velocity shown in Fig. 9 is calculated at the location of the dashed line.

surface heights in the Irminger Sea over the final 2 yr of integration are shown in Fig. 10. The ranges in sea surface height over the annual cycle for the three cases are 1.1 cm (deformation radius of 20 km), 2.2 cm (28 km), and 4.0 cm (40 km). The amplitude of the seasonal cycle increases approximately as the deformation radius squared. This is as expected from the quasigeostrophic theory in section 3 because the change in Ψ due to wind forcing is proportional to the stratification. The mean sea surface height also becomes increasingly negative with larger stratification. This is a result of the wind-driven circulation penetrating less deep and also a diminished influence of the bottom topography as the stratification increases. For very strongly stratified calculations, the bottom becomes isolated from the upper ocean and the westward flow separates from the coast at the southern tip of Greenland and follows the zonal potential vorticity contours all the way to the western boundary (not shown).

The choice of uniform stratification used in the model

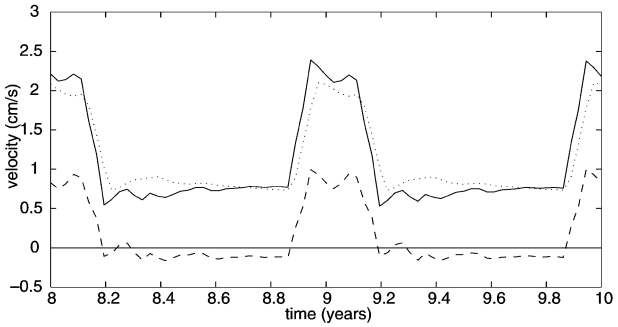

FIG. 9. Northward velocity at level 1 (solid) and near bottom at level 7 (dashed) under the region of forcing in the MIT model. The essential characteristics of the two-dimensional quasigeostrophic analytical model are reproduced in the full three-dimensional primitive equation model. The connection between the northward flow under the region of forcing and the strength of the recirculation is demonstrated by the eastward transport west of the forcing region (dotted line).

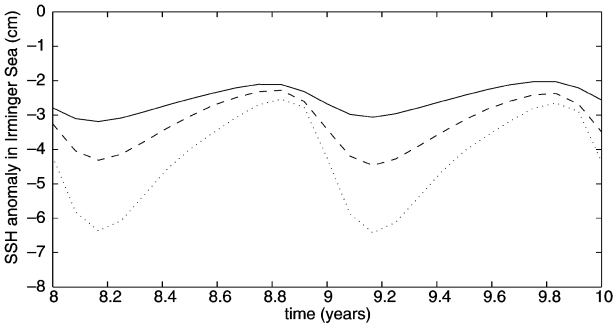

FIG. 10. Time series of the minimum sea surface height anomaly in the Irminger Sea for three calculations in which the first baroclinic deformation radius is: 20 (solid), 28 (dashed), and 40 km (dotted).

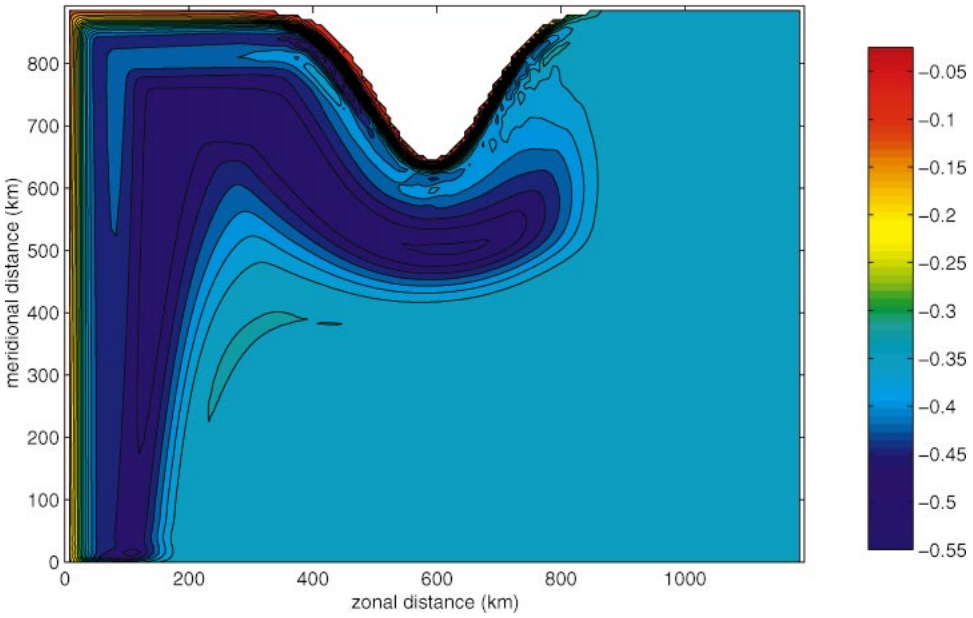

FIG. 11. Mean sea surface height anomaly (cm) for no stratification.

is made for simplicity and for direct comparison with the QG theory. The actual nonwinter stratification in the Labrador and Irminger Seas is not uniform with depth, but is enhanced near the surface and bottom with a local minimum at middepth (due to the convected mode water). We have carried out numerical calculations with realistic stratification based on observed temperature and salinity profiles and find results similar to those presented here but with somewhat stronger recirculation strengths.

The case of no stratification results in a very different mean circulation and seasonal cycle. The mean sea surface height for a barotropic calculation is shown in Fig. 11. The magnitude within the recirculation as compared with the basin interior is now an order of magnitude weaker than that with stratification (cf. Fig. 5). This is because the circulation feels the full effect of the bottom slope, which makes the gradient in potential vorticity very large in the region of forcing. The resulting Sverdrup circulation over the strongly sloping bottom, where topographic beta is orders of magnitude larger than planetary beta, is very weak. The seasonal cycle is in phase with the wind forcing (not shown). The absence of stratification removes the slow timescale associated with baroclinic Rossby waves from the problem and the adjustment is achieved by rapidly propagating barotropic Rossby waves, which transit the domain in less than 1 day. This rapid barotropic response is also present in the baroclinic calculations, but its amplitude is so small that it is negligible in comparison with the baroclinic signal.

The circulation and seasonal variability found in the primitive equation model also depend strongly on the bottom slope near the boundaries. The mean sea surface height with the standard coastline and stratification—but with a flat bottom—is shown in Fig. 12. The sea surface height in the Irminger Sea is very similar to that found with the sloping bottom. However, the recirculation into the Labrador Sea now extends westward, along latitude lines, from the southern tip of Greenland to the western boundary. Note that there is no overshoot to the south because the bottom is flat. Because the westward flow and eastward flow are now in closer proximity to each other, lateral viscosity causes more contours to close to the southwest of Greenland. There is also a vastly different seasonal cycle for the case of a flat bottom. The minimum sea surface height in the Irminger Sea varies by almost 6 cm from summer to winter compared to approximately 1 cm for the case with a sloping bottom (Fig. 13a). The signal in winter is much stronger because there is no compression at the bottom when the wind forcing is active to offset the stretching due to Ekman suction. The signal is greatly reduced in summer because the stretching at the sloping bottom provided by the westward Rossby wave propagation is absent. A similarly enhanced seasonal cycle is found in the eastward transport south of Greenland (Fig. 13b).

It is of interest to note that for a linear, stratified, inviscid system the steady circulation is independent of the bottom slope (Anderson and Killworth 1977). However, the primitive equation calculations presented here clearly show that the bottom topography influences the mean circulation. Essentially identical mean circulations result from steady forcing with the mean wind stress, so the difference from the linear theory is not related to the time-dependent forcing. However, as discussed by Young and Rhines (1982), weak dissipation can en-

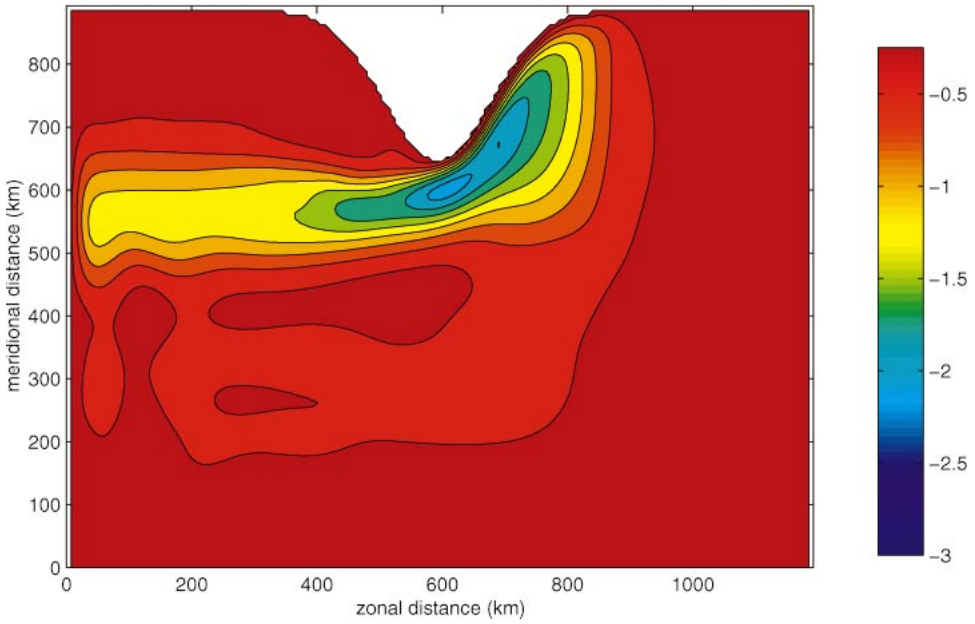

FIG. 12. Mean sea surface height anomaly (cm) from the final year of a 10-yr integration with a flat bottom.

hance the vertical scale of the flow and drive deep circulations. The vertical scale of the resulting circulation can be derived by assuming that the potential vorticity balance is nearly linear, $\beta V \approx f\partial w/\partial z$, and that the horizontal velocity is of the same order of magnitude as the baroclinic Rossby wave phase speed, $V = O(\beta L_d^2)$, as is observed. This results in an estimate for the vertical scale of the wind-driven flow as

$$H = \frac{fw}{\beta^2 L_d^2}, \tag{10}$$

where w is the vertical velocity at the base of the Ekman layer. For the mean wind stress curl to the east of Greenland, the Ekman suction velocity $w = O(10^{-5}\ \text{m s}^{-1})$. For parameters typical of the subpolar North Atlantic, $f = 10^{-4}\ \text{s}^{-1}$, $L_d = 20$ km, $\beta = 2 \times 10^{-11}\ \text{m}^{-1}\ \text{s}^{-1}$, (10) gives a vertical scale for the wind-driven circulation of $O(6000$ m). This is much greater than the water depth, and so it is expected that the wind-forced circulation will feel the bottom. Other scalings can be used (e.g., Young and Rhines 1982) that give similarly large vertical scales. Once the flow feels the bottom, the topographic beta becomes important and the flow follows the topography around the Labrador Sea. The calculations with increased stratification show that even doubling the deformation radius to 40 km does not isolate the bottom slope from the upper ocean, although it is clearly beginning to do so.

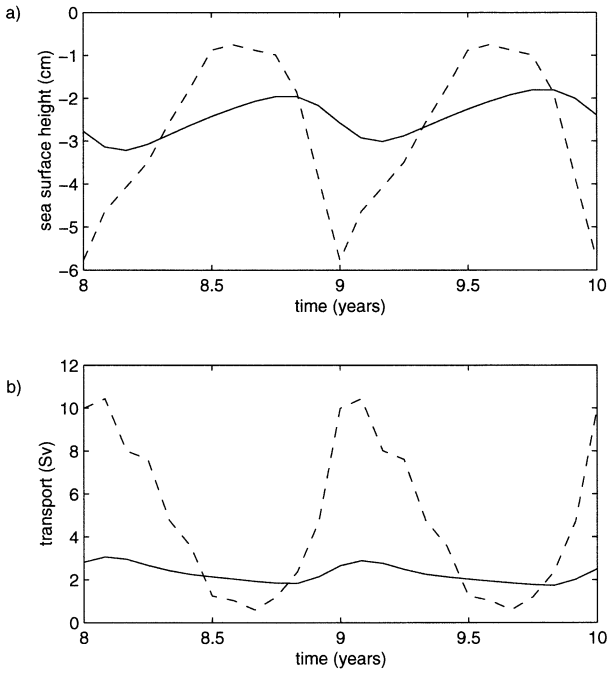

FIG. 13. Time series of (a) minimum sea surface height anomaly in the Irminger Sea and (b) eastward transport south of Greenland over the final 2 yr of integration with a flat bottom (dashed lines) and with topography (solid lines, as in Fig. 6).

These results, together with the aid of the simple theory in section 3, demonstrate the importance of the bottom slope and stratification in determining both the strength of the mean circulation and its modulation over the annual period. The combined influences of stratification, which introduces a slow timescale to the problem, and bottom topography, which provides a source of vorticity to the water column, are key to maintaining a nearly steady circulation throughout the year even though the forcing is localized and time dependent.

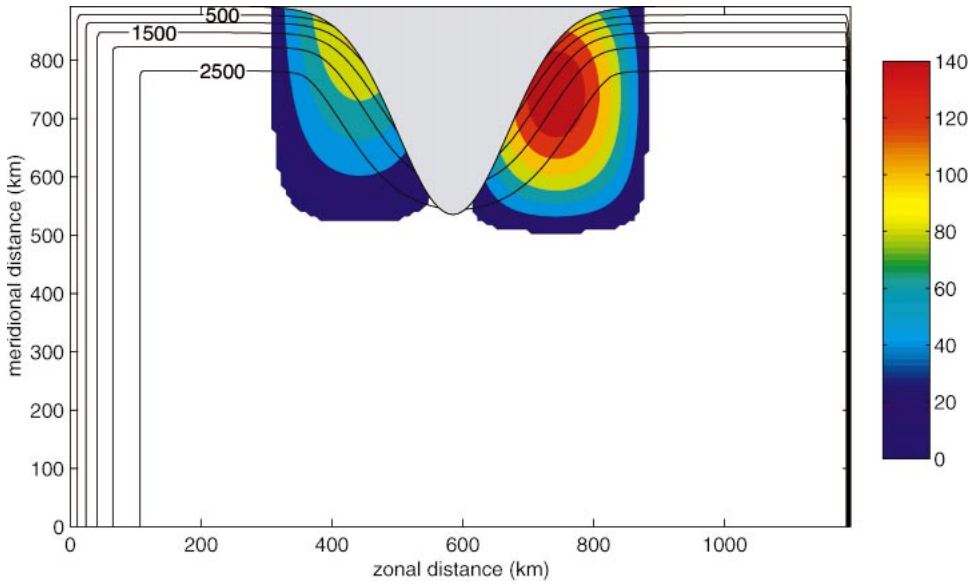

FIG. 14. Model bottom topography (contours) and wind stress curl (N $m^{-3} \times 10^{-8}$) with wind forcing added to the west of Greenland.

5. Recirculation in the Labrador Sea

The dynamic height field of Lavender et al. (2000) shows closed contours within the northern Labrador Sea (Fig. 1). Although there is some observational uncertainty, the spatial scale and magnitude of this feature suggest that it is reasonably well resolved by the float data. Our modeling and theoretical results thus far have produced closed contours only in regions where viscosity is active, to the south and east of Greenland and along the western boundary of the model domain. We touch on two likely mechanisms here that may be responsible for the Labrador recirculation gyre: local wind and eddy fluxes.

As noted earlier, the winter wind stress curl is also enhanced along the west coast of Greenland in the northeast Labrador Sea (although it is somewhat weaker and located over shallower topography; see Fig. 2). We have repeated the standard calculation with the addition of a patch of cyclonic wind stress curl along west Greenland, as shown in Fig. 14. The mean sea surface height resulting from this wind forcing is shown in Fig. 15. The cyclonic wind stress curl in the northern Labrador Sea drives a closed cyclonic recirculation gyre of $O(0.5)$ cm. This has a weaker transport than the recirculation in the float study, and it is also weaker than the larger-scale recirculation forced by the winds east of Greenland in the model.

Eddy kinetic energy estimates derived from altimetric data (Prater 2002; Lilly et al. 2003, manuscript submitted to *Progress in Oceanography*, hereinafter LRS), surface drifters (Fratantoni 2001), and subsurface float data (Lavender 2001) indicate that particularly strong eddy variability is found in the eastern Labrador Sea (Fig. 16). This suggests that eddy fluxes may be a possible driving source of the Labrador Sea recirculation (e.g., Rhines and Holland 1979). While there is also a band of enhanced variability along the east coast of Greenland, it is in very shallow water—hence it is unlikely that the Irminger recirculation gyre is driven by eddies. The source of the large eddy kinetic energy in the eastern Labrador Sea appears to be related to the formation of eddies from the boundary current near 61°N (LRS). At this location there is abruptly changing topography: to the south the continental slope is very steep and to the north it is much broader (Fig. 16). Thus, one possibility is that the localization of the eddy generation is related to the local topography (Eden and Böning 2002; Bracco and Pedlosky 2003).

While it is beyond the scope of this study to represent the boundary currents in their full complexity, the possible importance of eddy fluxes is crudely explored here by introducing a region of enhanced topographic slope along the west coast of Greenland, as shown in Fig. 17, for a calculation with wind forcing only to the east of Greenland. The steep continental slope west of Greenland results in closed contours in the northern Labrador Sea, qualitatively consistent with the pattern found in the float data. This is to be compared with the sea surface height in Fig. 5 for the calculation with standard topography. Note that there are now more closed contours to the south of Greenland as well, and so the recirculation in the Irminger Sea has become more isolated from the recirculation in the Labrador Sea.

Analysis of the potential vorticity budget indicates that the Labrador recirculation is driven by a lateral viscous flux of cyclonic vorticity from the boundary current into the interior. The boundary current is accelerated when it flows into the region of steep topog-

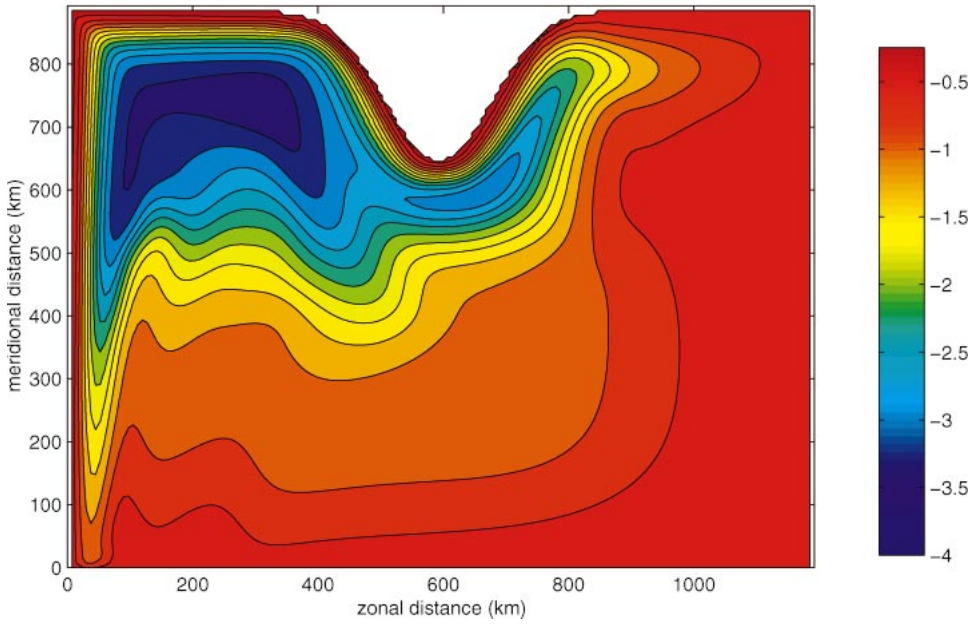

FIG. 15. Mean sea surface height anomaly (cm) from the final year of a 10-yr integration with wind stress curl added to the west of Greenland.

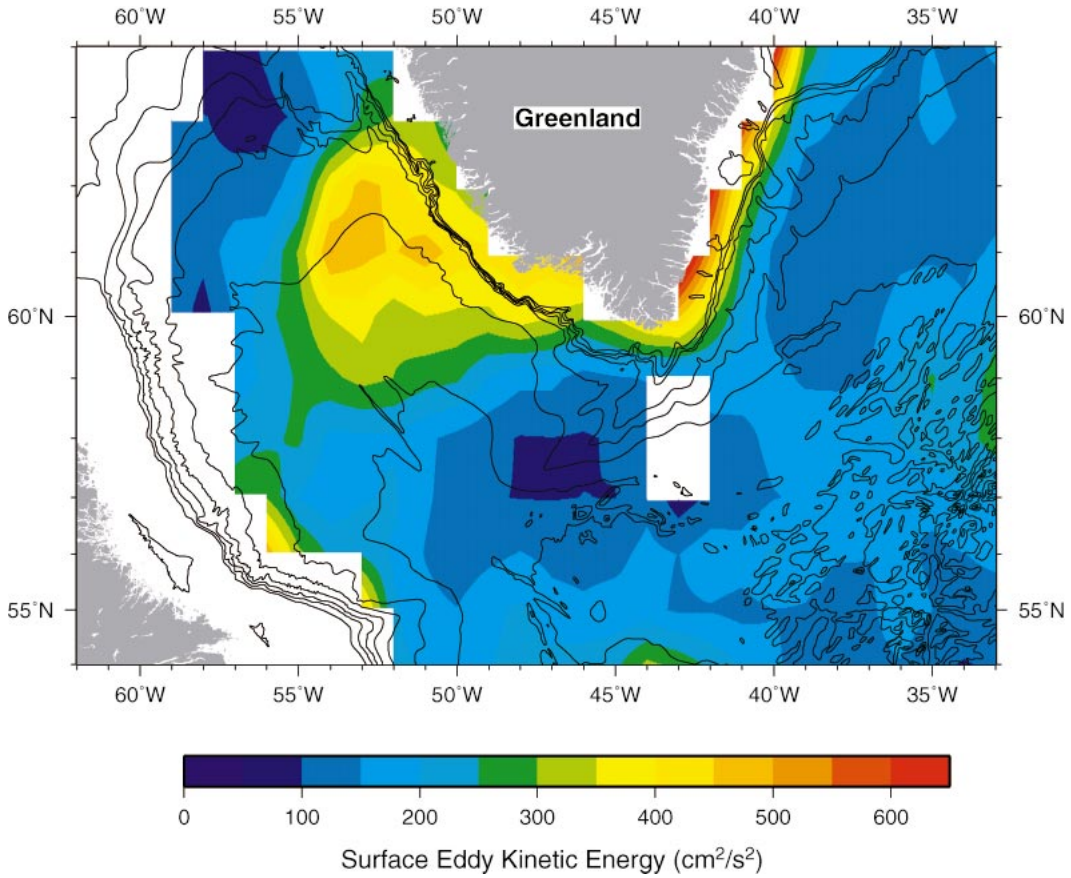

FIG. 16. Bottom topography showing the region of steep slope along the west coast of Greenland (bottom contours are 500–3500 m by 500-m increments) along with the surface eddy kinetic energy (after Fratantoni 2001).

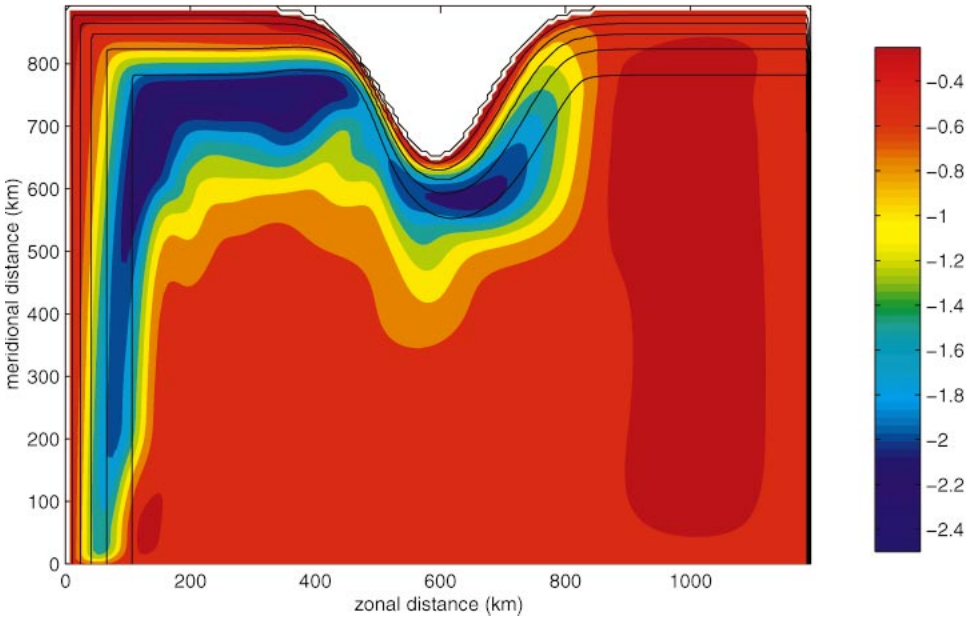

FIG. 17. Mean sea surface height anomaly (cm) over the final year of a 10-yr integration for a case with a steep topographic slope along west Greenland (color). The topography is indicated by the contours.

raphy as it tries to follow contours of f/h. This acceleration increases the cyclonic relative vorticity on the offshore side of the front. The model lateral viscosity diffuses this cyclonic vorticity offshore, where it drives the flow northward across planetary vorticity contours and forms the closed recirculation gyre. The increased number of closed contours south of Greenland also results from enhanced diffusion. Specifically, the eastward return flow (with lower potential vorticity) is adjacent to the westward flow over a greater distance than in the standard case (cf. Figs. 17 and 5).

Thus a closed recirculation in the northern Labrador Sea in the model may be driven by a lateral flux of high potential vorticity from the boundary current into the interior, localized in the region of steep topography. We note that in the eastern Labrador Basin the Irminger Current does have high potential vorticity compared to the interior as a result of both the cyclonic relative vorticity along the offshore side of the current and the enhanced stratification compared to that found in the interior. We view the eddy flux mechanism as more likely to be responsible for this feature than the forcing due to the enhanced curl west of Greenland. This is because the circulation produced by winds based on NCEP (and ECMWF) produce a gyre that is too weak and has larger meridional scale than found in the float data. The magnitude of the eddy potential vorticity flux in the real ocean is not known, but with even a weak source of high potential vorticity near the boundary in our model, and a means to flux that vorticity into the interior, we find a significant cyclonic recirculation. We emphasize that these results are somewhat speculative because the lateral viscosity used here is a very poor parameterization of the real eddy fluxes. Clearly more realistic studies need to be carried out to explore the impact of eddy formation along the west coast of Greenland on the circulation in the Labrador Sea.

6. Concluding remarks

We have argued that the cyclonic recirculation gyres recently observed in the Irminger and Labrador Seas are predominantly driven by the strong wind stress curl east of Greenland that develops every winter. An idealized primitive equation ocean model forced with such localized, seasonally varying winds produces mean recirculations that are in qualitative agreement with the observed gyres in terms of their strength, horizontal and vertical scales, and locations. Although the forcing is active only during winter, the resulting circulation is weakly time dependent. A simple two-layer quasigeostrophic theory demonstrated that the key to this persistence is the combined effect of weak stratification and the continental slope under the forcing region east of Greenland. Interactions with the bottom weaken the oceanic response during winter, when the wind is strong, and maintain the circulation throughout the summer, when the wind is weak. Topography also provides a wave guide along the boundary to transmit this circulation far from the forcing region into the western Labrador Sea. Additionally, there is also support for either local wind forcing or eddy fluxes along the west coast of Greenland to drive a smaller closed recirculation in the northern Labrador Sea.

Determining what forces these recirculation gyres is an important step toward understanding the general cir-

culation in the subpolar North Atlantic and its low frequency variability. Hydrographic evidence suggests that the recirculation gyres are preferential sites for deep convection and water mass transformation in both the Labrador and Irminger Seas (Pickart et al. 2003b). Furthermore, trapping of parcels within these recirculations may lead to an interannual variability of deep-water formation and export that is not simply related to the local (in space or time) atmospheric conditions. The eastward return flow south of Greenland also provides a direct advective link between the region of deep convection in the Labrador Sea and the Irminger Sea. Although idealized, we feel that the results described here provide a simple but illuminating view of the essential dynamics of these recently observed recirculation gyres.

Acknowledgments. This work was supported by the National Science Foundation under Grant OCE-0095060. Kara Lavender is thanked for providing the estimate of the eastward transport south of Greenland in the PALACE float data. Kent Moore generously provided the NCEP reanalysis fields and answered numerous questions regarding weather analysis products.

REFERENCES

Adcroft, A., C. Hill, and J. Marshall, 1997: Representation of topography by shaved cells in a height coordinate ocean model. *Mon. Wea. Rev.,* **125,** 2293–2315.

Anderson, D. L. T., and P. D. Killworth, 1977: Spin-up of a stratified ocean with topography. *Deep-Sea Res.,* **24,** 709–732.

Bracco, A., and J. Pedlosky, 2003: Vortex generation by topography in locally unstable baroclinic flows. *J. Phys. Oceanogr.,* **33,** 207–219.

Clarke, R. A., and J. C. Gascard, 1983: The formation of Labrador Sea Water. Part I: Large-scale processes. *J. Phys. Oceanogr.,* **13,** 1764–1778.

Eden, C., and C. Böning, 2002: Sources of eddy kinetic energy in the Labrador Sea. *J. Phys. Oceanogr.,* **32,** 3346–3363.

Fratantoni, D. M., 2001: North Atlantic surface circulation during the 1990's observed with satellite-tracked drifters. *J. Geophys. Res.,* **106,** 22 067–22 093.

Käse, R. H., A. Biastoch, and D. B. Stammer, 2001: On the mid-depth circulation in the Labrador and Irminger Seas. *Geophys. Res. Lett.,* **28,** 3433–3436.

Lavender, K. L., 2001: The general circulation and open-ocean deep convection in the Labrador Sea: A study using subsurface floats. Ph.D. thesis, University of California, San Diego, 131 pp.

——, R. E. Davis, and W. B. Owens, 2000: Mid-depth recirculation observed in the interior Labrador and Irminger Seas by direct velocity measurements. *Nature,* **407,** 66–69.

Lazier, J. R. N., and D. G. Wright, 1993: Annual velocity variations in the Labrador Current. *J. Phys. Oceanogr.,* **23,** 559–678.

Madec, G., F. Lott, P. Delecluse, and M. Crepon, 1996: Large-scale preconditioning of deep-water formation in the northwestern Mediterranean Sea. *J. Phys. Oceanogr.,* **26,** 1393–1408.

Marshall, J., and F. Schott, 1999: Open-ocean convection: Observations, theory, and models. *Rev. Geophys.,* **37,** 1–64.

——, C. Hill, L. Perelman, and A. Adcroft, 1997a: Hydrostatic, quasi-hydrostatic, and nonhydrostatic ocean modeling. *J. Geophys. Res.,* **102,** 5733–5752.

——, A. Adcroft, C. Hill, L. Perelman, and C. Heisey, 1997b: A finite-volume, incompressible Navier-Stokes model for studies of the ocean on parallel computers. *J. Geophys. Res.,* **102,** 5753–5766.

McCartney, M. S., and L. D. Talley, 1982: The subpolar mode water of the North Atlantic Ocean. *J. Phys. Oceanogr.,* **12,** 1169–1188.

Milliff, R. F., and J. Morzel, 2001: The global distribution of the time-average wind stress curl from NSCAT. *J. Atmos. Sci.,* **58,** 109–131.

Pedlosky, J., 1996: *Ocean Circulation Theory.* Springer, 453 pp.

Pickart, R. S., D. J. Torres, and R. A. Clarke, 2002: Hydrography of the Labrador Sea during active convection. *J. Phys. Oceanogr.,* **32,** 428–457.

——, M. A. Spall, M. H. Nielsen, R. F. Milliff, and G. W. K. Moore, 2003a: Deep convection in the Irminger Sea forced by the Greenland tip jet. *Nature,* in press.

——, F. Straneo, and G. W. K. Moore, 2003b: Is Labrador Sea Water formed in the Irminger Basin? *Deep-Sea Res.,* **50A,** 23–52.

Prater, M., 2002: Eddies in the Labrador Sea as observed by profiling RAFOS floats and remote sensing. *J. Phys. Oceanogr.,* **32,** 411–427.

Renfrew, I. A., G. W. K. Moore, P. S. Guest, and K. Bumke, 2002: A comparison of surface-layer heat flux and surface momentum flux observations over the Labrador Sea with ECMWF analyses and NCEP reanalyses. *J. Phys. Oceanogr.,* **32,** 383–400.

Rhines, P. B., and W. R. Holland, 1979: A theoretical discussion of eddy-driven mean flows. *Dyn. Atmos. Oceans,* **3,** 289–325.

Smith, E. H., F. M. Soule, and O. Mosby, 1937: The Marion and General Greene expeditions to Davis Strait and Labrador Sea. Scientific results, Part 2: Physical oceanography. *Bull. U.S. Coast Guard,* **19,** 1–259.

Spall, M. A., 2000: Buoyancy-forced circulations around islands and ridges. *J. Mar. Res.,* **58,** 957–982.

Stommel, H. M., 1982: Is the South Pacific helium-3 plume dynamically active? *Earth Planet. Sci. Lett.,* **61,** 63–67.

Straneo, F., R. S. Pickart, and K. Lavender, 2003: Spreading of Labrador Sea Water: An advective–diffusive study. *Deep-Sea Res.,* in press.

Sy, A., M. Rhein, J. R. N. Lazier, K. P. Koltermann, J. Meincke, A. Putzka, and M. Bersch, 1997: Surprisingly rapid spreading of newly formed intermediate waters across the North Atlantic Ocean. *Nature,* **386,** 675–679.

Talley, L. D., and M. S. McCartney, 1982: Distribution and circulation of Labrador Sea Water. *J. Phys. Oceanogr.,* **12,** 1189–1205.

Trenberth, K., J. Olson, and W. Large, 1989: A global windstress climatology based on ECMWF analyses. Tech. Rep. NCAR/TN-338 + STR, 93 pp.

Young, W. R., and P. B. Rhines, 1982: A theory of the wind-driven circulation II. Gyres with western boundary layers. *J. Mar. Res.,* **40,** 849–872.